Supporting information

Tunable doping of graphene by physisorbed self-assembled networks

Roald Phillipson,[a] *César J. Lockhart de la Rosa,*[bc] *Joan Teyssandier,*[a] *Peter Walke,*[a] *Deepali Waghray,*[a] *Yasuhiko Fujita,*[a] *Jinne Adisoejoso,*[a] *Kunal S. Mali,*[a] *Inge Asselberghs,*[c] *Cedric Huyghebaert,*[c] *Hiroshi Uji-i,*[ad] *Stefan De Gendt* [ce] *and Steven De Feyter* [a*]

[a] KU Leuven-University of Leuven, Department of Chemistry, Division of Molecular Imaging and Photonics, Celestijnenlaan 200F, B-3001 Leuven, Belgium

[b] KU Leuven, Department of Metallurgy and Materials Engineering, Kasteelpark Arenberg 44, B-3001 Leuven, Belgium

[c] imec, Kapeldreef 75, B-3001 Leuven, Belgium

[d] RIES, Hokkaido University, Sapporo, 001-0020, Japan

[e] KU Leuven-University of Leuven, Department of Chemistry, Division of Molecular Design and Synthesis, Celestijnenlaan 200F, B-3001 Leuven, Belgium

*Corresponding authors

Email: steven.defeyter@kuleuven.be, Stefan.DeGendt@imec.be

Synthesis of nonacosylamine (NCA)

NMR spectra were acquired on a commercial instrument (Bruker Avance II 600 MHz) and chemical shifts (δ) are reported in parts per million (ppm) referenced to tetramethylsilane (^{1}H). Chemicals received from commercial sources (Acros Organic and Sigma-Aldrich) were used without further purification. All solvents were used as received from commercial sources and not explicitly dried prior to use ($H_2O \leq 0.1\%$).

Synthesis of nonacosylamine: To a solution of melissic acid (0.500 g, 1.1 mmol) in chloroform (20 mL), concentrated H_2SO_4 (3.0 mL, 55.0 mmol) was added and the mixture was heated to 50 ºC. Sodium azide (0.360 g, 5.53 mmol) was slowly added to the above mixture over a period of 2h. Following the addition, the mixture was heated and stirred at 50 ºC for another 2h. The lower acidic layer was separated and poured into an ice bath (15 mL). The resulting suspension was heated to 80 ºC and was treated with 10N NaOH until a pH of 11.0. The crude product was extracted with chloroform. The organic layers were combined and evaporated and the product was recrystallized from an ethanol/ether mixture and dried under vacuum. **Nonacosylamine** (0.100 g, 22 %) was obtained as a white solid. ^{1}H NMR (600 MHz, $CDCl_3$): δ 2.67 (t, J = 6.9 Hz, 2H, CH_2NH_2), 1.48-1.41 (m, 2H, $CH_2CH_2NH_2$), 1.28-1.25 (m, 52H, alkyl-CH_2), 0.88 (t, J = 6.6 Hz, 3H, CH_3).

Self-assembly of ODA and NCA on HOPG: effect of annealing

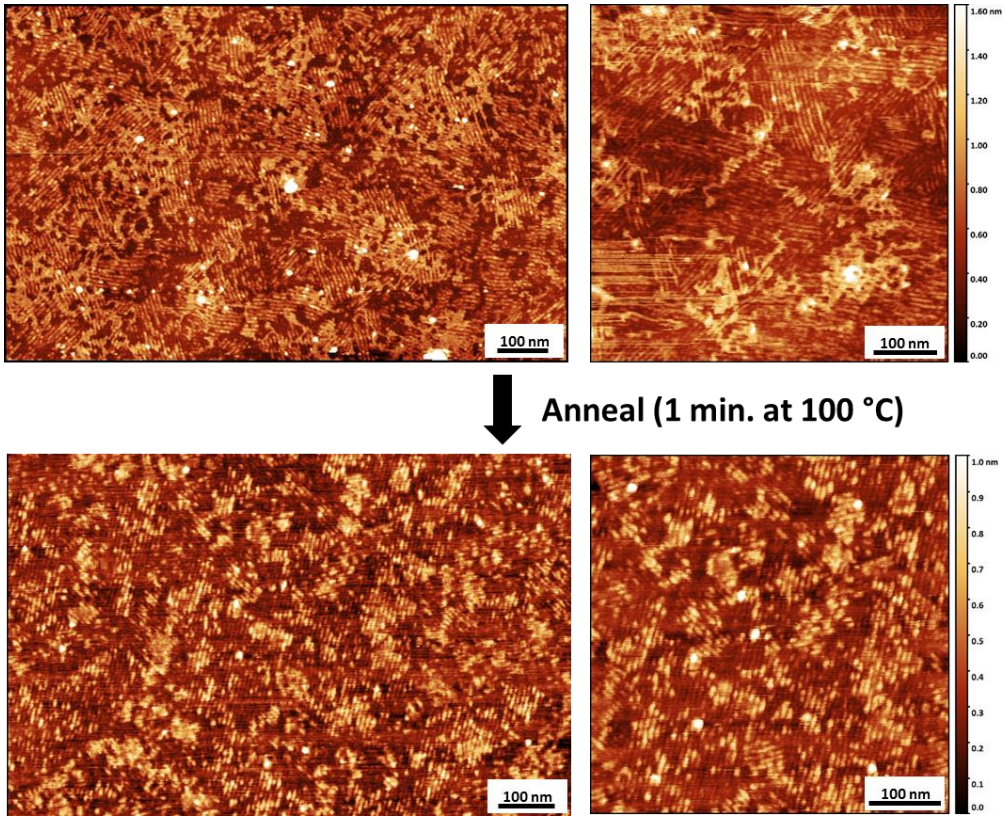

Figure S1. AFM topography images of a dip coated NCA film on HOPG. Large scale and high resolution images before (top part) and after (bottom part) annealing on a hot plate.

To ensure an optimal quality of the self-assembled layers on HOPG, annealing (1 min at 100 °C on a hot plate) of the samples was systematically performed, as well as AFM imaging before and after. In the case of NCA (figure S1), full surface coverage is obtained after dip coating, but the annealing step gives a greater homogeneity and better ordering. In the case of ODA (figure S2), the effect is more dramatic. The domain size is considerably enlarged (leading to domains extended over several hundreds of nanometers), reducing drastically the proportion of domain boundaries. In addition, there is a homogenization in film thickness due to rearrangement and/or sublimation of the molecules from the surface. A brief annealing improves therefore substantially the quality and ordering of the films by reducing the density of defects and improving their homogeneity. It leads to samples with an optimized density of amine functions on the surface.

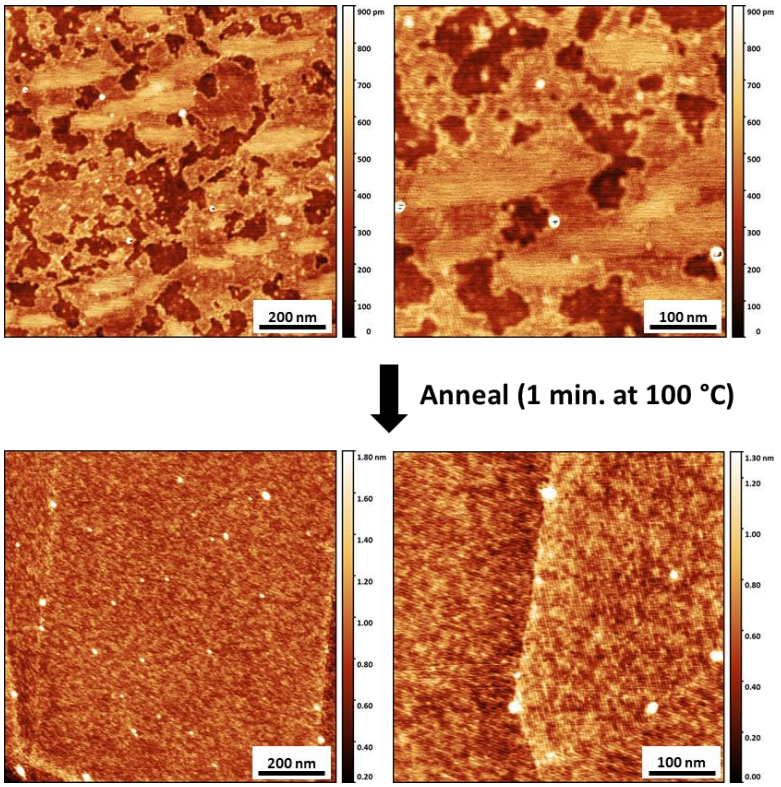

Figure S2. AFM topography images of a dip-coated ODA film on HOPG. Large scale and high resolution images before (top part) and after (bottom part) annealing on a hot plate.

CVD graphene transferred to SiO_2: effect of cleaning with toluene

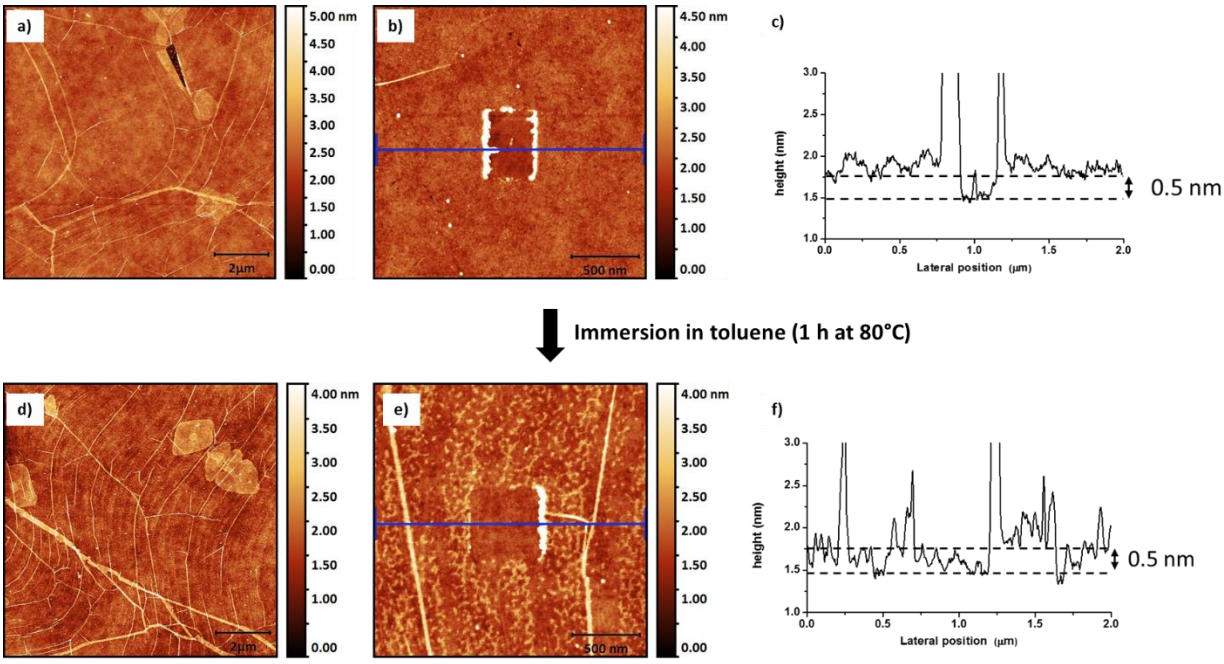

Figure S3. AFM topography images of CVD graphene on SiO_2, before and after toluene clean. (a) Image of graphene on SiO_2 as received from Graphenea. (b) Image from the same area as (a) where a 500×500 nm^2 area was scratched with an AFM tip to determine the thickness of the contamination layer. (c) Height profile taken along the blue line in panel (b). (e) Image from the same area as (d) where a 500×500 nm^2 area was scratched with an AFM. (f) Height profile taken along the blue line in panel (e).

One of the main issues of CVD graphene compared to HOPG is its cleanliness, particularly after the transfer process to SiO_2 that introduces polymeric contamination. It requires therefore a reliable cleaning protocol. Before assessing the effect of cleaning by a solvent (namely toluene), it is important to develop a way to quantify the amount of contamination present on graphene. For this purpose, mechanical cleaning was performed on samples with an AFM tip. The graphene was first imaged in tapping mode on a large scale. Then, a 500 x 500 nm^2 area was imaged in contact mode with a force of 20 nN (scan rate of 1 Hz, with 100 points per line, *i.e.*, a line per 5 nm), which results in removal of the molecules on top of graphene within this area. Later, the same area was

imaged again in tapping mode to measure the thickness of the contamination film. The same AFM cantilever was used throughout the process.

As can be seen in figure S3a, the graphene surface looks initially homogeneous. After scratching, it appears that there is in fact a 0.5 nm thick layer of contamination present on top, as measured in the height profile in figure S3c, showing the difference between the cleaned graphene and the rest of the sample (homogenously covered by contaminants). The very bright region at the edges of the scratched square in figure S3b correspond to an accumulation of molecules scratched away from the square. When performed on a sample cleaned by immersion in hot toluene (see figure S3d-f), scratching still evidences the presence of this 0.5 nm thick contamination, but it appears now discontinuous over the surface, proving that large parts of the polymer have been removed by toluene. Immersion in hot toluene provides thus an easy and non-aggressive way to reduce contamination on graphene.

Methodology for correcting Raman data for bilayer spots and defects

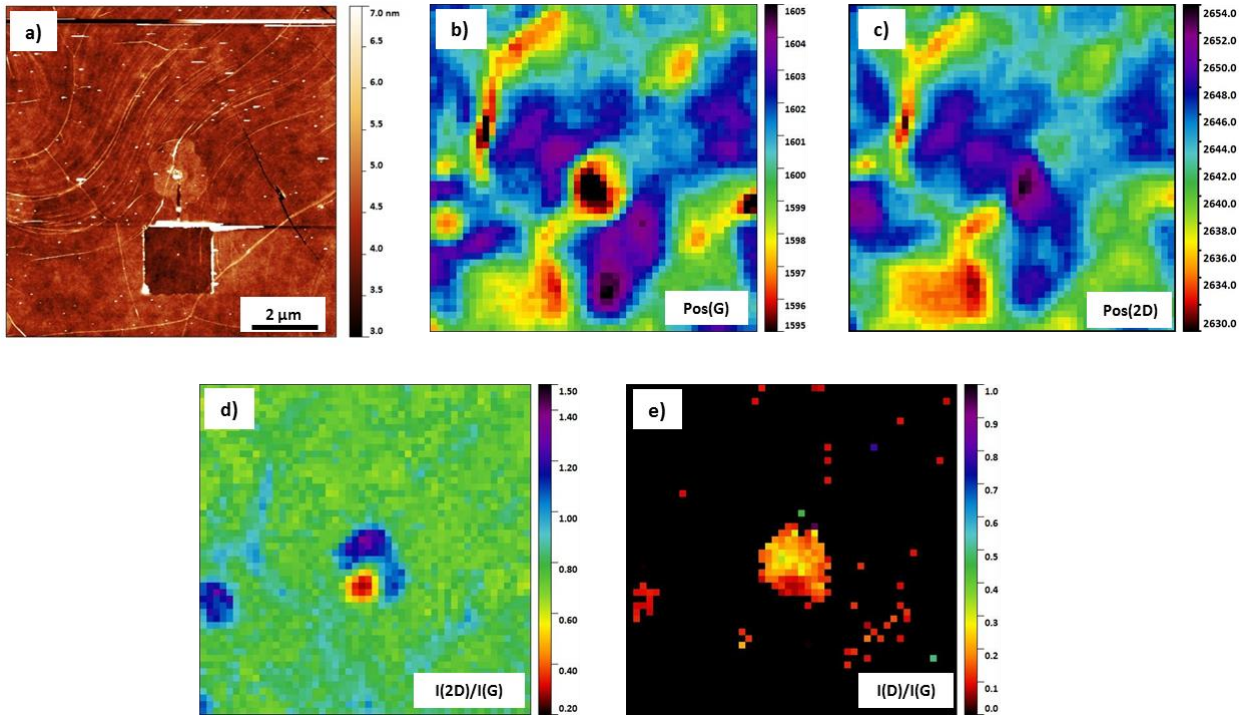

Figure S4. Correlation of the spatial variation in Raman signals with the structural features of graphene. (a) AFM image of CVD grown graphene transferred to SiO_2. (b-e) Raman maps acquired in the same area showing the spatial variation of Pos(G), Pos(2D), I(2D)/I(G) and I(D)/I(G).

Bilayer spots and defects present on the graphene surface affect the Raman spectrum thereby hampering the analysis of molecular doping. To investigate the effect of these features, Raman spectroscopy and AFM were carried out on CVD graphene on SiO_2 at the same location. In addition, the effect of scratching with the AFM tip on the properties of graphene was investigated. In the AFM image of graphene shown figure S4a, bilayer spots are visible in the middle and to the left, surrounded by several wrinkles. Below the bilayer spot a 2×2 μm^2 area was scratched with the AFM tip using the same method discussed above thereby removing polymer residues originating from the transfer process (the graphene was not cleaned using toluene). Figures S4b, S4c, S4d and S4e show Raman maps (50×50 pts^2) of the Pos(G), Pos(2D), I(2D)/I(G) and I(D)/I(G), respectively, obtained in the same area as the AFM image. Comparing the images, AFM scratching has no effect on the Raman features, demonstrating that the technique is non-destructive and that the polymer residues do not have a large contribution on the amount of doping. There is a large variation in Pos(G) and Pos(2D) over the area which can be related to variation in strain and at the bilayer spot there is a large downshift of Pos(G) and upshift of Pos(2D). The bilayer spot is also clearly visible in the I(2D)/I(G) map. Interestingly, I(2D)/I(G) at the bilayer spot is partly upshifted and downshifted compared to single layer graphene, which is related to the relative orientation of the graphene layers. While Bernal stacked bilayer graphene has a lower intensity ratio compared to single layer graphene, turbostratic graphene has a higher intensity ratio.[1] Also, there is a higher D peak at the bilayer spot due to edge states and/or defects. For correctly interpreting molecular doping it is thus necessary to isolate data points having an outlying I(2D)/I(G) and I(D)/I(G).

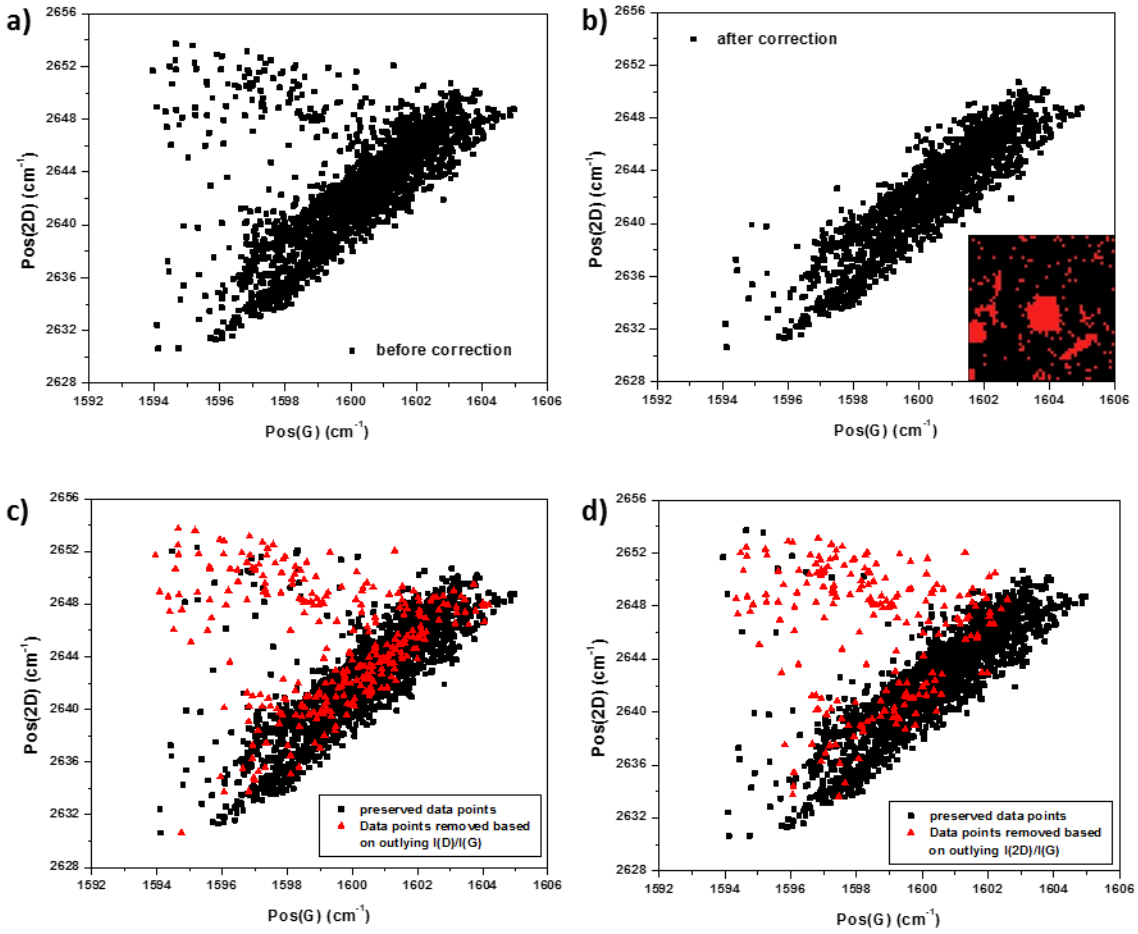

Figure S5. Correction of Raman data obtained on CVD grown graphene based on data points corresponding to outlying I(D)/I(G) and I(2D)/I(G). (a,b) Plots of Pos(2D) *versus* Pos(G) before and after data correction, inset in (b) shows a map were the red pixels correspond to removed data points. (c,d) Plots of Pos(2D) *versus* Pos(G) showing the data points that are removed based on outlying I(D)/I(G) and I(2D)/I(G).

To remove data points that correspond to bilayer graphene and defects, the following conditions are used: data points are removed if I(D)/I(G)>0.1 and/or if I(2D)/I(G) is more than 3 median absolute deviations away from the median. Figure S5a shows a plot of Pos(2D) *versus* Pos(G) corresponding to Raman maps shown above. Most data points are aligned along a line with a gradient of 2.2 which correspond to variation in strain. However, outliers are present with a

upshifted Pos(2D) in relation to data points that follow the strain line. When the conditions for outlier removal are applied to this data set, almost all outliers are removed, see figure S5b.

Raman control experiments: effects of dip coating CVD grown graphene in pure solvent

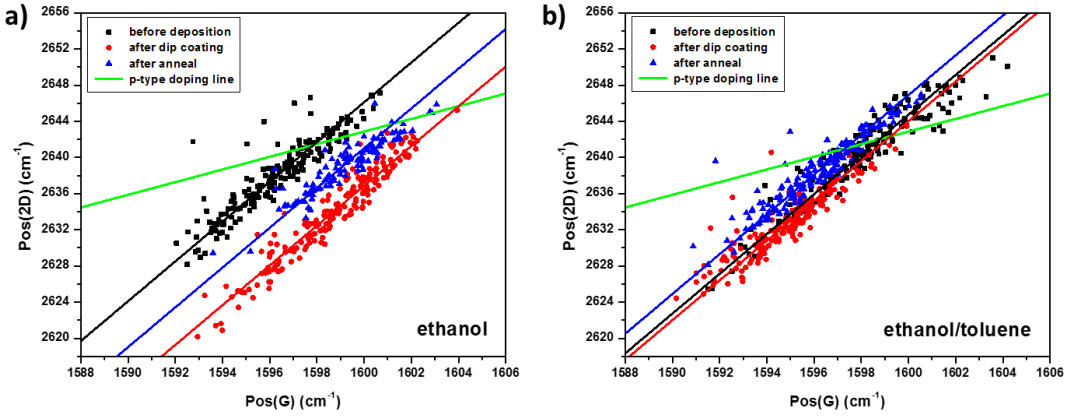

Figure S6. Effect of immersion of graphene in solvent on doping. (a,b) Plots of Pos(2D) *versus* Pos(G) showing the doping effect of immersion in ethanol and ethanol/toluene.

To exclude interference from the solvents used for deposition of the dopants on the characterization of molecular doping, the effect of immersing graphene in the solvents was investigated using Raman spectroscopy. The exact same protocol for immersion was used as for deposition of the compound (30 min. immersion and withdraw at 1 mm/min). After immersion in ethanol, Pos(G) shifts to higher wavenumbers indicating p-type doping, see figure S6a. Possibly this effect is caused by trace amounts of ethanol or impurities left on the surface after drying or by structural rearrangement of the graphene film during immersion.[2] Annealing the sample for 1 min at 100 °C resulted in a small reduction of p-type doping. In contrast to pure ethanol, immersion in a mixture of ethanol and toluene (50/50 v/v %) did not result in a significant change in doping, and again subsequent annealing did result in reduction of p-type doping, see figure S6b. Based on these experiments it can be concluded that the solvent did not contribute to the n-type doping effect seen after functionalization with NCA or ODA.

Mechanical cleaning of devices using AFM

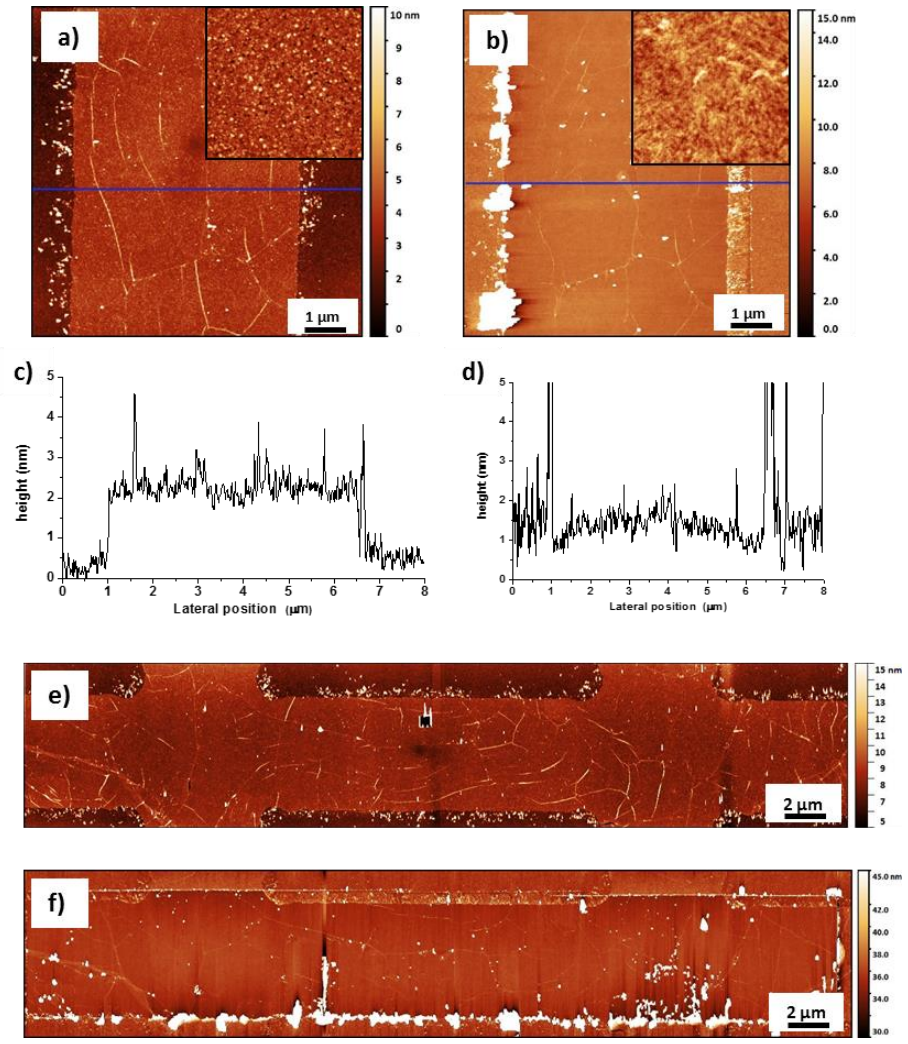

Figure S7. Mechanical cleaning of graphene devices using AFM. (a) AFM image of a device channel before cleaning, inset shows zoomed in area (1×1 μm^2). (b) AFM image of the same area in (a) after mechanical cleaning using AFM, inset shows zoomed in area (1×1 μm^2). (c) Height profile corresponding to blue line in (a). (d) Height profile corresponding to blue line in (b). (e) AFM image of entire channel before cleaning. (f) AFM image of entire channel after cleaning.

The amount of contamination on the device channels originating from the device fabrication process was characterized using AFM. The AFM image and the corresponding height profile shown in figure S7a and S7c shows that there is at least a ≈2 nm thick contamination layer on top of the channel. Because it is very challenging to remove this contamination fully using standard wet cleaning methods or thermal annealing at high temperatures without damaging graphene, AFM scratching was utilized to mechanically sweep away the polymer residues. AFM scratching was done in AFM contact mode with a soft cantilever (2 N/m) at a rate of 1 Hz and a force of ≈20 nN. After cleaning, the majority of the residue is removed from the channel and swept away to the SiO_2 substrate, see figure S7b and figure S7b, and The RMS roughness was reduced from 0.82 to 0.19 nm. Using this method the entire channel between the potential probes can be cleaned, see figure S7e and S7f, giving a pristine surface suitable for self-assembly.

Effect annealing on the electrical characteristics of devices functionalized with ODA and NCA *via* dip coating

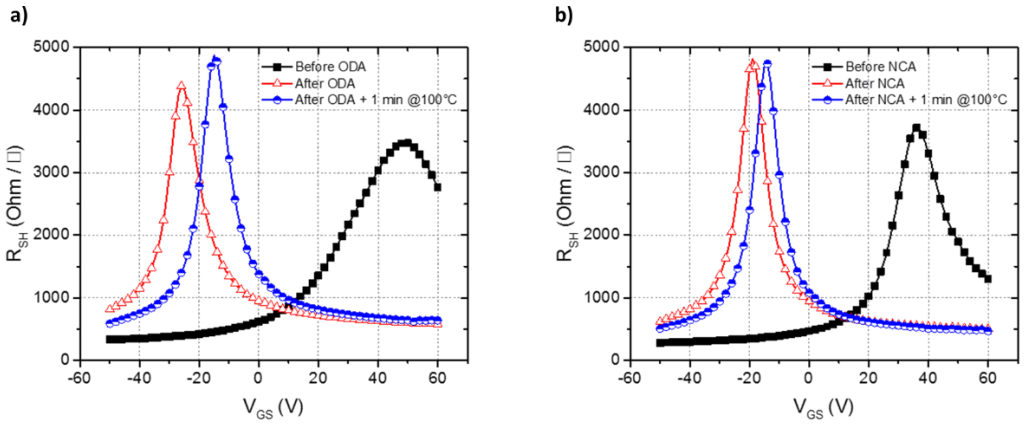

Figure S8. Effect of annealing on the electric transport of devices functionalized with self-assembled networks. Both for devices functionalized with ODA (a) and NCA (b) there is an upshift of V_k after annealing that could be explained by desorption of dopant molecules from the surface.

After the functionalized devices (4-probe devices 1 and 2) were cleaned by immersion in toluene, thermal annealing and AFM, they were functionalized again with ODA and NCA *via* dip coating. The shift of V_k upon functionalization was 76 V for ODA and 55 V for NCA and the ratio of these shifts is 1.38. The ratio is lower than the expected 1.6, this difference can be explained by a small difference in layer thickness of the molecular film or contamination. The different V_k before functionalization, 49 V for device 1 and 36 V for device 2, suggests that device 1 was more contaminated than device 2. In accordance with the Raman measurements there is reduction in n-type doping after annealing (1 min on a hot plate at 100 °C), likely because of desorption of dopant molecules from the surface. Interestingly the shift of the NCA functionalized device (5V) is lower than the shift of the ODA functionalized sample (11V). This observation is in agreement with the expected lower thermal stability for the shorter chain length molecule.

Self-assembly on graphene field-effect devices

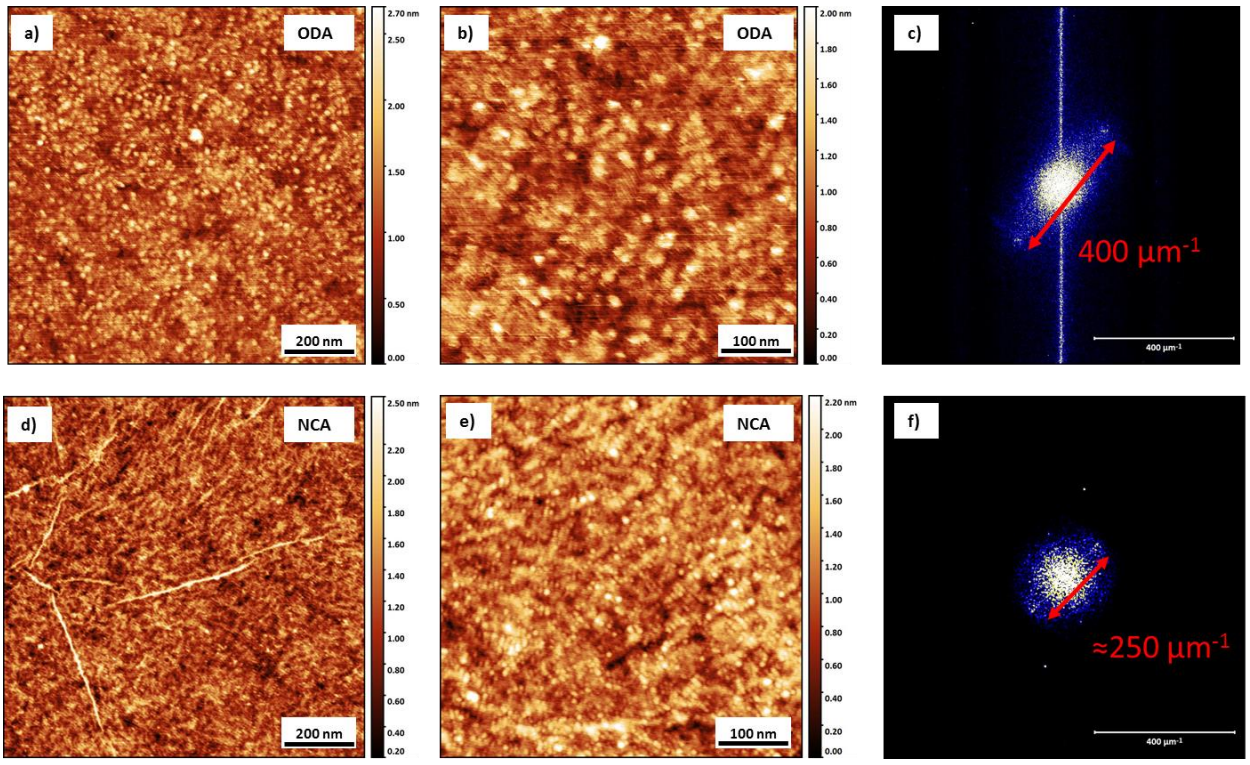

Figure S9. Structural characterization of self-assembly of ODA and NCA on graphene devices using AFM (a,b) AFM topography images of a dip coated ODA film on a scratched graphene device. (c) Fourier transform of the image in b. (d,e) AFM topography images of a dip-coated

NCA film on a scratched graphene device. (f) Fourier transform of the image in e. All images have been recorded on samples annealed for 1 min on a hot plate at 100 °C.

The graphene field-effect devices were functionalized using the usual protocol (dip-coating and post-annealing). In order to demonstrate that this method leads also to self-assembled layers on devices, AFM imaging was performed on the scratched devices. The figures S9a and b shows the topography of ODA films on such samples. It can be seen, particularly for the smaller scale image, that the lamellar organization of the molecules observed on HOPG and CVD graphene is present over the entire device. Due to the corrugation of graphene, the quality of the organization is not as good as on HOPG, but the films exhibit less defects and higher domain sizes than those prepared on CVD graphene. The scratching cleaning method improves thus the quality of subsequent self-assembly. The periodicity measured from the Fourier transform (5 nm) matches well with the value measured on HOPG, and confirms the nature of the self-assembled layer. A similar observation can be made for NCA films (figure S9d and e). They exhibit homogeneous self-assembly over the device and the periodicity (8 nm) is in very good agreement with NCA self-assembled layers on HOPG. This data shows that a nice self-assembly can even be obtained on the devices and demonstrates that the density of doping functional groups as well as their tunability can be controlled and correlated with the electrical measurements.

Extracted parameters of electrical devices

All the additionally extracted parameters of the analyzed devices can be seen in table S1.

Table S1. Device parameters before and after functionalization with ODA or NCA.

	DEVICE	K POINT (V)	N_{2D} (cm^{-2})	μ_E ($cm^2V^{-1}s^{-1}$)	μ_H ($cm^2V^{-1}s^{-1}$)
UNDOPED (A)	1_11	50	1.19E+13	NA	1658
	1_15	57	1.35E+13	NA	789
	1_21	50	1.19E+13	NA	1500
	1_24	51	1.21E+13	NA	1549
A + ODA	1_11	-22	-5.23E+12	2327	1192
	1_15	-19	-4.52E+12	1058	495
	1_21	-18	-4.28E+12	1934	1102
	1_24	-20	-4.75E+12	2024	1076
UNDOPED (A)	2_11	43	1.02E+13	NA	1734
	2_13	59	1.40E+13	NA	395
	2_14	53	1.26E+13	NA	456
	2_15	54	1.28E+13	NA	939
A + NCA	2_11	5	1.19E+12	2153	555
	2_13	10	2.38E+12	511	95
	2_14	5	1.19E+12	621	130
	2_15	20	4.75E+12	1020	220
AFM clean (B)	1_14	17	4.04E+12	1325	333
	2_24	18	4.28E+12	1525	496
B + ODA	1_14	-30	-7.13E+12	1455	1530
B + NCA	2_24	-13	-3.09E+12	2322	1106

References

1. Lenski, D. R.; Fuhrer, M. S., Raman and Optical Characterization of Multilayer Turbostratic Graphene Grown Via Chemical Vapor Deposition. *J. Appl. Phys.* **2011,** *110,* 013720.
2. Klar, P.; Casiraghi, C., Raman Spectroscopy of Graphene in Different Dielectric Solvents. *Phys. Status Solidi C* **2010,** *7,* 2735-2738.